

Received August 19, 2019, accepted September 12, 2019, date of publication October 8, 2019, date of current version February 4, 2020.

Digital Object Identifier 10.1109/ACCESS.2019.2945976

# Sliding Mode Compensation Control for Diaphragm Tension in Unwinding Process of Lithium Battery Diaphragm Slitting Machine

CHENG JIANG<sup>1</sup>, HENG-SHENG WANG<sup>1,2</sup>, LI-WEI HOU<sup>1</sup>, AND LIANG-LIANG JIANG<sup>1</sup>

<sup>1</sup>College of Mechanical and Electrical Engineering, Central South University, Changsha 410083, China

<sup>2</sup>State Key Laboratory for High Performance Complex Manufacturing, Central South University, Changsha 410083, China

Corresponding author: Heng-Sheng Wang (whsheng@csu.edu.cn)

This work was supported in part by the Major State Basic Research Development Program of China under Grant 2013CB035504, and in part by the ShenZhen Gade Equipment Technology Co., Ltd.

**ABSTRACT** In order to solve the problem of tension control in the actual unwinding process of the lithium battery diaphragm slitting machine, the dynamic model of diaphragm and slitting machine unwinding system is constructed in this paper based on the diaphragm deformation in the unwinding system during the sampling period, in view of the nonlinear system characteristics of the unwinding system and the unstable diaphragm tension caused by the uncertain interference and the inaccurate model in the unwinding process. Considering the unwinding system characteristics of multi-output and strong coupling between outputs, a multi-variable comprehensive sliding surface for balancing unwinding diaphragm tension and unwinding speed, and a sliding mode controller for controlling the diaphragm tension in unwinding process are designed. And the stability of the sliding surface and the controller is proved. The fault-tolerant improvement of the sliding mode controller is carried out for practical engineering application, and the differential tracking disturbance observer is proposed to quickly estimate and compensate the external disturbance of the system. Finally, the results of the comparative experiments verify the effectiveness of the proposed diaphragm tension control scheme.

**INDEX TERMS** Lithium battery diaphragm slitting machine, tension control, sliding mode control, differential tracking disturbance observer.

## I. INTRODUCTION

Lithium batteries play a significant role in the new energy field, and one of whose key inner components is the diaphragm. The lithium battery diaphragm slitting machine(LBDSM) is an industrial equipment that slits a large-diameter, large-width lithium battery diaphragm roll into small-diameter, small-width one. During the slitting process, the diaphragm tension and speed are two key factors to ensure product quality [1]. Unwinding is the core part of the slitting machine, and one of its main objectives is to achieve the expected diaphragm transmission speed, while control the tracking error caused by diaphragm tension within a certain range. Due to the change of winding diameter and moment of inertia of the diaphragm roll with time, as well as the influence of friction, roller layout and other uncertain factors In the process of unwinding. The unwinding system

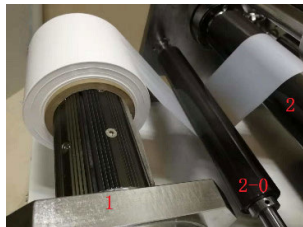
has become a complex electromechanical system with multiple input, multiple output, nonlinear, strong coupling and strong interference. Diaphragm tension control is difficult. The physical diagram of the unwinding system of LBDSM is shown in Fig. 1.

With the developing in high speed and high precision of LBDSM, the distributed PI type controllers which is often used in industrial winding systems can not meet the production requirements [1]. Therefore, scholars have conducted a lot of research in related fields. In terms of model perfection and roller control, an longitudinal dynamic model of the web is developed by [2], [3]. In [4], an air entrainment model of web-winding systems has been studied and the influence of air entrainment on the web tension fluctuation was explained by simulation analysis. Using Whitworth's model for span tension dynamics, the role of active dancers in tension control of webs is discussed in [5]. Control the web tension of web-winding systems by controlling the dancer roller with the  $H_\infty$  controller is discussed in [1]. Dynamics and control

The associate editor coordinating the review of this manuscript and approving it for publication was Valentina E. Balas .



(a)



(b)



(c)

**FIGURE 1.** The LBDMS used in this paper (a) whole machine; (b) side view of unwinding system; (c) top view of unwinding system.

of accumulators in continuous strip processing lines was considered in [6]. The role of dancers in attenuation of tension disturbances was studied in [7], [8]. In terms of systematic control algorithms, for the web tension control system, a method of overlapping decomposition is proposed in [9], and it is pointed out that a disjoint decomposition may deteriorate the control performance due to the mutual interactions, and the overlapping decompositions could improve the performance. In [10], 2DOF  $H_\infty$  control algorithm was applied to the web-winding system. A robust centralized H controller for a web winding system was proposed in [11]. Web tension controller of web-winding system based on neural network has been studied in [12], [13]. And the [14] present multivariable decentralized  $H_\infty$  controllers with one or two degrees of freedom, with and without explicit integrator, applied to winding systems, and two different controller structures are considered: a centralized controller and semi-decentralized controllers with or without overlapping. In practical applications, friction and disturbance are important factors affecting the control performance of the system, therefore, an approach that considers issues such as friction compensation and disturbance rejection was proposed in [15]. In [16], an observer with friction and inertia compensation was presented, which enables sensorless measurement and control of web tension of web-winding systems. A disturbance observer based approach for web tension control of roll-to-roll processing was proposed in [17]. And [18] employed an iterative learning control method for parallel structure to suppress the periodic disturbance due to friction in a roll-to-roll tension control problem. Reference [19] estimates the web tension that is considered to be disturbed by the disturbance observer, develops an iterative learning sliding mode controller. Sliding mode control methods have been widely and continuously

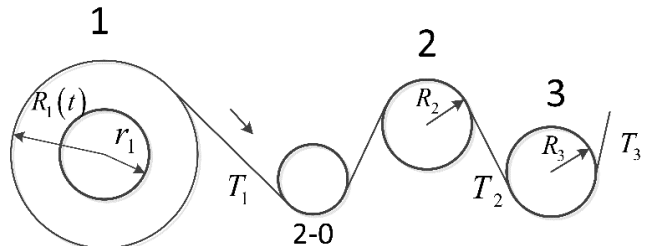


**FIGURE 2.** Schematic diagram of unwinding system of LBDMS.

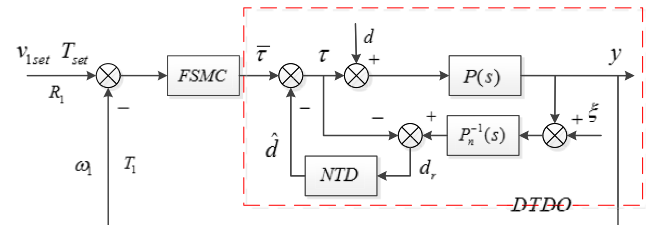


**FIGURE 3.** System control block diagram.

studied and applied in various fields because of its robustness and convergence [20]–[22]. However, the above papers are only theoretical analysis and simulation, the control object is not the same as this article, the experimental results can not meet the control requirements of the LBDMS, experimental environment is too simplified, or only a single tension expectation control experiment is performed, which is difficult to prove the adaptability of the control scheme. In summary, the methods in the above papers are difficult to apply directly to the actual production control of the LBDMS mentioned in this paper.

To solve the diaphragm tension control problem in the actual unwinding process of LBDMS, the mathematical model of the unwinding system of LBDMS shown in Fig. 2 is established according to the working principle of the actual LBDMS, and the decentralized control strategy is adopted [2], [10]. For the torque control of unwind motor, the sliding mode controller is designed based on the Lyapunov function as the stability criterion in this paper. Based on this sliding mode controller, the designed controller is improved according to the actual working condition of the slitting machine, which improves its fault tolerance in actual work. Meanwhile, the differential tracking disturbance observer based on differential tracker is designed to estimate and compensate the unknown external disturbance during the operation of the system (the system block diagram is shown in Fig. 3). Finally, the experimental results show that the fault-tolerant sliding mode controller (FSMCDTDOC) with differential tracking disturbance observer compensation has good control performance on the diaphragm tension in the unwinding system. Since the main speed roller only needs to generate the reference speed of the unwinding system, the classical PID control can achieve good control performance, so the control algorithm will not be described in detail herein.

## II. SYSTEM MODELING

Fig.2 shows the unwinding system of LBDSM. Roller 1 is a motor-driven unwind roller, the inner radius of the lithium battery diaphragm roll wound on the roller 1 is  $r_1$ , The outer radius of the diaphragm roll is  $R_1(t)$ , which is time-varying during the unwinding process. Roller 2 is load cell roller with a radius of  $R_2$  for measuring diaphragm tension. Roller 3 is the master speed roller, which produces the reference transmission speed of diaphragm, the outer layer is made of rubber, radius is  $R_3$ . The maximum static friction between the diaphragm and roller 3, which isolates the diaphragm tension on both sides of the main speed roller within a certain tension range, so that the control of the diaphragm tension (the diaphragm tension between the rollers 1 and 3) in the unwinding system is relatively independent. Roller 2-0 is a transfer roller, which is used to fix the wrap angle of the diaphragm on the load cell roller, and prevent the measurement error caused by direction change of the combined force of the diaphragm tension on both sides of the load cell roller. The effect of the roller 2-0 on the diaphragm tension of the unwinding system is considered to be a disturbance, and the dynamics model of the roller 2-0 will not be described again since its dynamic model is the same as the load cell roller.

### A. UNWIND SECTION

According to Newton's second law of motion, the dynamic equation of the unwind section is as follows

$$\tau_1 - Md_1 + \frac{T_1 \cdot R_1(t)}{j_1} - \frac{b_1 \omega_1}{j_1} = \frac{d}{dt}(J_1 \cdot \omega_1 j_1) \quad (1)$$

where  $j_1$  is the gearing ratio between the motor shaft and unwind roll shaft,  $\omega_1$  is the angular velocity of unwind roller,  $\tau_1$  is the electromagnetic torque of unwind motor,  $b_1$  is the coefficient of friction in the unwind roll shaft [2],  $J_1$  is the inertia of all elements on the unwind section converted onto the unwind motor shaft,  $T_1$  is the diaphragm tension in the span between the unwind roller and the load cell roller,  $Md_1$  is the damping torque converted onto the unwind motor shaft.

Considering the dynamic process, at any time  $t$ , the moment of inertia of the unwind section that is converted to the unwind motor shaft is as follows

$$J_1(t) = J_m + \frac{1}{j_1^2}[J_c + J_{\omega 1}(t)] \quad (2)$$

where  $J_m$  is the inertia of all the rotating elements on the motor side, which includes inertia of motor armature, driving pulley (or gear), driving shaft, etc.,  $J_c$  is the inertia of the driven shaft and the core mounted on it,  $J_{\omega 1}(t)$  is the inertia of the cylindrically wound diaphragm material on the core, Both  $J_m$  and  $J_c$  are constants, but the inertia  $J_{\omega 1}(t)$  is not constant because the diaphragm is continuously released into the process. The inertia  $J_{\omega 1}(t)$ , is given by

$$J_{\omega 1}(t) = \frac{\pi}{2}H\rho(R_1^4(t) - r_1^4) \quad (3)$$

where  $H$  is width of diaphragm,  $\rho$  is density of diaphragm. In order to stabilize the diaphragm tension, it is necessary to

keep the velocity of the diaphragm coming off the unwind roll unchanged, when the velocity of the diaphragm coming on the load cell roll is fixed, because the strong coupling between the transmission speed of the diaphragm and the diaphragm tension in the unwinding system, that is, the line speed of the unfolding diaphragm at the unwinding end is constant. Due to the constant change of the outer radius of the diaphragm roll, the angular velocity of the unwind roll is also constantly changing. Therefore, in order to reduce the computational complexity in the control process, the following formula group replacement is performed:

$$\begin{cases} \omega_1 = \frac{v_1}{R_1(t)} \\ \dot{\omega}_1 = \frac{\dot{v}_1}{R_1(t)} - \frac{v_1 \dot{R}_1(t)}{R_1^2(t)} \end{cases} \quad (4)$$

In the unit time of unwinding process

$$\dot{R}_1(t) \approx \frac{-hv_1}{2\pi R_1(t)} \quad (5)$$

where  $h$  is the thickness of diaphragm,  $v_1$  is the velocity of the diaphragm coming off the unwind roll.

Simultaneous formula (1)-(5), we get

$$\begin{aligned} \tau_1 = & \left( \frac{j_1 J_1}{2\pi R_1^3(t)} - \frac{\rho H R_1(t)}{j_1} \right) v_1^2 h + \frac{j_1 J_1}{R_1(t)} \dot{v}_1 \\ & + \frac{b_1 v_1}{j_1 \cdot R_1(t)} - \frac{T_1 \cdot R_1(t)}{j_1} + M d_1 \end{aligned} \quad (6)$$

The quadratic term of the linear velocity and the time-varying  $R_1(t)$  make the unwinding system a variable-parameter nonlinear system, which increases the complexity of the diaphragm tension control.

### B. LOAD CELL ROLL SECTION

$$J_2 \cdot \frac{d\omega_2}{dt} = (T_2 - T_1)R_2 - \mu r_2[G_2 - (T_1 + T_2) \times \cos(\pi - \Phi/2)] \quad (7)$$

where  $J_2$  is the inertia of the load cell roller,  $T_2$  is the diaphragm tension in the span between the load cell roller and the master speed roller,  $\mu$  is the coefficient of friction in the load cell roll bearing,  $r_2$  is the inner radius of the load cell roll bearing,  $\Phi$  is the wrap angle of the diaphragm on the load cell roller,  $G_2$  is the total weight of rotating parts such as rollers, bearing outer rings and other accessories.

Because the inertia and friction of the load cell roller are relatively small in practical engineering applications, the influence of the load cell roller on the unwinding system is regarded as disturbance, which can be overcome by improving the anti-interference performance of the designed controller.

### C. MASTER SPEED ROLLER SECTION

The dynamic equation of the master speed roller is

$$J_3 \frac{d(\omega_3 j_3)}{dt} = \tau_3 - M d_3 - \frac{(T_2 - T_3)R_3 + b_3 \omega_3}{j_3} \quad (8)$$

where  $j_3$  is the gearing ratio between the motor shaft and master speed roll shaft,  $\omega_3$  is the angular velocity of master speed roller,  $\tau_3$  is the electromagnetic torque of master speed motor,  $b_3$  is the coefficient of friction in the master speed roll shaft,  $J_3$  is the inertia of all elements on the master speed roll that is converted to the master speed motor shaft,  $T_3$  is the diaphragm tension on the underside of the main speed roller,  $Md_3$  is the damping torque that is converted to the master speed motor shaft.

#### D. DYNAMICS MODEL OF LITHIUM BATTERY DIAPHRAGM

Ignoring the influence of the load cell roller, that is,  $T_1 = T_2$ . According to Hook's theorem and the quality conservation, during the sampling period  $\Delta t$ , the shape-variation relationship of diaphragm in the span between the unwinding roller and the main speed roller is as follows:

$$\frac{L}{E \cdot A} \cdot T_1(t + \Delta t) = \frac{L}{E \cdot A} \cdot T_1(t) + v_3 \cdot \Delta t - v_1 \cdot \Delta t \\ + v_1 \cdot \Delta t \cdot \frac{T_0}{E \cdot A} - v_3 \cdot \Delta t \cdot \frac{T_1(t)}{E \cdot A} \quad (9)$$

where  $T_1(t)$  is the value of  $T_1$  at time  $t$ ,  $T_1(t + \Delta t)$  is the value of  $T_1$  at time  $(t + \Delta t)$ ,  $T_0$  is original tension of the diaphragm in the diaphragm roll,  $E$  is the modulus of elasticity of the diaphragm material,  $A$  is the area of cross section of the diaphragm,  $L$  is the length of the web span between unwind roller and master speed roller,  $v_3$  is the velocity of the diaphragm coming on the master speed roller, that is, the linear speed of the master speed roller, ignore the influence of the load cell roller and the slip phenomenon.

From (9), we derive:

$$\frac{T_1(t + \Delta t) - T_1(t)}{\Delta t} = \frac{E \cdot A(v_3 - v_1)}{L} + v_1 \cdot \frac{T_0}{L} - v_3 \cdot \frac{T_1(t)}{L}$$

When  $\Delta t \rightarrow 0$ :

$$\frac{T_1(t + \Delta t) - T_1(t)}{\Delta t} \approx \dot{T}_1(t)$$

Then the diaphragm dynamics equation is

$$\dot{T}_1 = -\frac{T_1}{L} \cdot v_3 + \frac{E \cdot A \cdot (v_3 - v_1)}{L} + \frac{v_1}{L} \cdot T_0 \quad (10)$$

Under equilibrium, that is  $T_1(t + \Delta t) = T_1(t)$ , the tension of the diaphragm is

$$T = E \cdot A \cdot \left(1 - \frac{v_1}{v_3}\right) + \frac{v_1}{v_3} \cdot T_0 \quad (11)$$

The Laplace transform of (10) is

$$T_1(t) = e^{-\frac{v_3}{L}t} \cdot T(0) + \left(1 - e^{-\frac{v_3}{L}t}\right) \\ \times \left[E \cdot A \cdot \left(1 - \frac{v_1}{v_3}\right) + \frac{v_1}{v_3} \cdot T_0\right] \quad (12)$$

where  $T(0)$  is the initial value of the  $T_1$ .

From the above analysis of the diaphragm dynamics model, it is known that there is a strong coupling between the transmission speed of the diaphragm and the diaphragm

tension, and the effect of the change in speed on the tension is delayed, and the delay time is determined by  $v_3$ . When the elastic modulus and cross-sectional area of the diaphragm are constant, the ratio of  $v_1$  to  $v_3$  determines the tension of the diaphragm under equilibrium.

The dynamics model of unwinding system is as follows:

$$\begin{cases} \tau_1 = \left( \frac{j_1 J_1}{2\pi R_1^3(t)} - \frac{\rho H R_1(t)}{j_1} \right) v_1^2 h + \frac{j_1 J_1}{R_1(t)} \dot{v}_1 \\ \quad + \frac{b_1 v_1}{j_1 \cdot R_1(t)} - \frac{T_1 \cdot R_1(t)}{j_1} + M d_1 \\ \dot{T}_1 = -\frac{T_1}{L} \cdot v_3 + \frac{E \cdot A \cdot (v_3 - v_1)}{L} + \frac{v_1}{L} \cdot T_0 \\ \tau_3 = J_3 \frac{d \left( \frac{j_3 v_3}{R_3} \right)}{dt} + \frac{(T_2 - T_3) R_3^2 + b_3 v_3}{j_3 R_3} + M d_3 \end{cases} \quad (13)$$

In practical engineering applications, the eccentricity and non-roundness of the diaphragm roll, the mounting error of the parts, and the measurement error of the sensor will all affect the operation of the unwinding system. The built dynamic model cannot fully and accurately represent kinetic characteristics of the unwinding system. Therefore, a control method insensitive to disturbance and model uncertainty is needed to improve the control accuracy and stability of the diaphragm tension in the unwinding system.

### III. SLIDING MODE CONTROLLER DESIGN

The strong robustness is an important advantage of sliding mode control, that is, it has excellent insensitivity to the model error of the controlled object, the change of the object parameters and the external disturbance [23]. In this paper, a sliding mode controller for diaphragm tension control is designed and its stability is judged by Lyapunov function.

#### A. THEORETICAL DESIGN OF SLIDING MODE CONTROLLER

Since the unwinding system has a system characteristic of multiple outputs and strong coupling between outputs, it is difficult to achieve overall stability of the system with a single output as a control object. Therefore, in the sliding surface design process of the sliding mode controller, it is necessary to comprehensively consider the control of the diaphragm unwinding tension and the unwinding speed to finally achieve stable and robust control of the diaphragm tension in unwinding process.

From (10), when the unwinding system reaches the desired value

$$\dot{T}_{set} = -\frac{T_{set}}{L} \cdot v_3 + \frac{E \cdot A \cdot (v_3 - v_{1set})}{L} + \frac{v_{1set}}{L} \cdot T_0$$

Equation (10) is subtracted from the above equation, we get:

$$\Delta \dot{T} = -\frac{\Delta T}{L} \cdot v_3 - \frac{\Delta v_1 \cdot E \cdot A}{L} + \frac{\Delta v_1}{L} \cdot T_0 \quad (14)$$

where  $\Delta v_1 = v_1 - v_{1set}$ ,  $\Delta T = T_1 - T_{set}$ ,  $v_{1set}$  and  $T_{set}$  are expected speed and tension, and from (11), we get:

$$v_{1set} = \frac{(T_{set} - EA) \cdot v_3}{T_0 - EA} \quad (15)$$

For system (14), Consider  $v_3$  as a constant, design  $\Delta v_1$  to make  $\Delta T = 0$  robust and stable. Select  $V = (1/2)(\Delta T)^2 > 0$  as the Lyapunov function candidate, then, when  $\Delta v_1 = -k\Delta T$  and  $k \leq v_3/(EA - T_0)$ , the derivative of  $V$  along (14), as follows:

$$\dot{V} = \Delta T \cdot \Delta \dot{T} = \left( -\frac{v_3}{L} + k \cdot \frac{E \cdot A - T_0}{L} \right) \Delta T^2 \leq 0 \quad (16)$$

The system is stable [24]. Where  $k$  is coefficient.

Then the multivariable integrated sliding surface can be designed as follows

$$s = \Delta v_1 + k \Delta T = 0 \quad (17)$$

And the derivative of equation (17) as follows

$$\dot{s} = \Delta \dot{v}_1 + k \Delta \dot{T} \quad (18)$$

From (6), we get

$$\begin{aligned} \dot{v}_1 &= (\tau_1 - Md_1) \frac{R_1(t)}{j_1 J_1} - \left( \frac{1}{2\pi R_1^2(t)} - \frac{\rho H R_1^2(t)}{j_1^2 J_1} \right) \\ &\quad \times v_1^2 h - \frac{b_1 v_1}{j_1^2 \cdot J_1} + \frac{T_1 \cdot R_1^2(t)}{j_1^2 \cdot J_1} \end{aligned} \quad (19)$$

In order to make the control method insensitive to uncertain factors such as inaccurate model of unwinding system, variation of model parameter and external disturbance, and play a good regulation and control role, this paper selects the trending law of sliding mode control [25], as follows:

$$\sigma = -\varepsilon \cdot \text{sgn}(s) - \beta \cdot s \quad (20)$$

where  $\varepsilon > 0$ ,  $\beta > 0$ . By adjusting the parameters  $\varepsilon$  and  $\beta$ , it is possible to ensure the dynamic quality of the sliding mode arrival process and to reduce the high frequency jitter of the control signal [25].

Let

$$\dot{s} = \Delta \dot{v}_1 + k \Delta \dot{T} = \sigma \quad (21)$$

Substituting the formulas (14) and (19) into the above formula, we get the control law as follows:

$$\begin{aligned} \tau_1 &= x_1 + x_2 + x_3 + x_4 \\ x_1 &= \left( \frac{j_1 J_1}{2\pi R_1^3(t)} - \frac{\rho H R_1(t)}{j_1} \right) v_1^2 h + \frac{b_1 v_1}{j_1 \cdot R_1(t)} \\ &\quad - \frac{T_1 \cdot R_1(t)}{j_1} + Md_1 \\ x_2 &= \frac{\dot{v}_{1set} \cdot j_1 \cdot J_1}{R_1(t)} \end{aligned}$$

$$x_3 = k \cdot \left( \frac{\Delta T}{L} \cdot v_3 + \frac{E \cdot A \cdot \Delta v_1}{L} - \frac{\Delta v_1}{L} \cdot T_0 \right) \cdot \frac{j_1 \cdot J_1}{R_1(t)}$$

$$x_4 = [-\varepsilon \cdot \text{sgn}(s) - \beta \cdot s] \cdot \frac{j_1 \cdot J_1}{R_1(t)} \quad (22)$$

During the unwinding system to achieve the required diaphragm tension, the unwinding roller and the main speed roller have acceleration processes of acceleration  $a_1$  and  $a_3$ , so the speed will be  $v_1 = a_1 t$  and  $v_3 = a_3 t$ . From equation (11), in order to make the tracking error of the tension zero, it is necessary to keep  $v_1/v_3 = i$  constant, then the acceleration process needs to:

$$\begin{cases} \frac{a_1 t}{a_3 t} = i, & t > 0 \\ i = \frac{T_{set} - EA}{T_0 - EA} \end{cases} \quad (23)$$

That is

$$\dot{v}_{1set} = a_1 = a_3 \cdot \frac{T_{set} - EA}{T_0 - EA} \quad (24)$$

For the sliding surface (17), choose the Lyapunov function candidate as follows:

$$V = \frac{1}{2} s^2 \quad (25)$$

Taking the control law (22), formula (18) and (24) into account, the derivative of (25) along (17), as follows:

$$\dot{V} = s \dot{s} = -\varepsilon \cdot s \cdot \text{sgn}(s) - \beta \cdot s^2 \leq 0 \quad (26)$$

The system is stable [24].

The proof of the trending law that allows the system to reach the sliding surface (20) within a limited time is as follows.

Suppose the initial state  $s(0) > 0$ , the process from the initial state to the sliding surface is:

$$\dot{s} = -\varepsilon - \beta \cdot s$$

Solving differential equations for the above formula, we get:

$$s = \left[ s(0) + \frac{\varepsilon}{\beta} \right] e^{-\beta t} - \frac{\varepsilon}{\beta}$$

Let

$$\left[ s(0) + \frac{\varepsilon}{\beta} \right] e^{-\beta t} - \frac{\varepsilon}{\beta} = 0$$

The time required for the system to reach the sliding surface  $s = 0$  from the initial state is

$$t = \frac{\ln[\varepsilon + \beta s(0)] - \ln(\varepsilon)}{\beta} \quad (27)$$

When the initial state is  $s(0) < 0$ , the same reason can be obtained as follows:

$$t = \frac{\ln[\varepsilon - \beta s(0)] - \ln(\varepsilon)}{\beta}$$

In actual engineering applications, the value of  $\varepsilon$ ,  $\beta$ , and  $s(0)$  has an upper limit, so the system can reach the sliding surface within a limited time.

In summary, the sliding mode control law of the unwinding system is as follows:

$$\begin{aligned}\tau_1 &= x_1 + x_2 + x_3 + x_4 \\ x_1 &= \left( \frac{j_1 J_1}{2\pi R_1^3(t)} - \frac{\rho H R_1(t)}{j_1} \right) v_1^2 h + \frac{b_1 v_1}{j_1 \cdot R_1(t)} \\ &\quad - \frac{T_1 \cdot R_1(t)}{j_1} + M d_1 \\ x_2 &= a_3 \cdot \frac{T_{set} - EA}{T_0 - EA} \cdot \frac{j_1 \cdot J_1}{R_1(t)} \\ x_3 &= k \cdot \left( \frac{\Delta T}{L} \cdot v_3 + \frac{E \cdot A \cdot \Delta v_1}{L} - \frac{\Delta v_1}{L} \cdot T_0 \right) \cdot \frac{j_1 \cdot J_1}{R_1(t)} \\ x_4 &= [-\varepsilon \cdot \text{sgn}(s) - \beta \cdot s] \cdot \frac{j_1 \cdot J_1}{R_1(t)} \quad (28)\end{aligned}$$

Through the above control law, the system states will converge to the desired equilibrium point follow the sliding mode surface in finite time.

## B. ENGINEERING APPLICATION IMPROVEMENT OF SLIDING MODE CONTROLLER

1) In the theoretical design, when the diaphragm tension  $T_1$  is less than the expected tension due to disturbance and other factors after the system is started, ie  $\Delta T < 0$ , it can be known from equations (11) and (15) that the  $v_1$  will be greater than the expected line speed  $v_{1set}$ , ie  $\Delta v_1 > 0$ , then  $s > 0$ , this will trigger the controller adjustment mechanism, ie  $\sigma < 0$ , the torque calculation value is reduced, the unwind motor is decelerated, thereby causing the system state to reach the sliding surface  $s = 0$ . Conversely, unwind motor acceleration. In this practical engineering application, the  $v_1$  is calculated by measuring the angular velocity of unwind motor and the radius of diaphragm roll, and the diaphragm winding tension is measured by the load cell roller (roller 2 in Fig. 2). Due to errors in component mounting and sensor measurement, the measured real-time linear velocity  $v_1$  and diaphragm tension  $T_1$  cannot accurately reflect the true value, which can cause the sliding surface to be in an unknown state, for example, during system operation, when the system is in the vicinity of the  $s = 0$ ,  $\Delta T < 0$ , due to measurement errors such as  $\Delta v_1 \leq 0$ ,  $s$  is in an unknown state, namely  $s \geq 0$  or  $s \leq 0$ , the system will not be able to accurately achieve  $\Delta T = 0$ . In order to solve the above problems, this paper has made fault-tolerant improvement on the sliding surface, as follows

$$\begin{aligned}\Delta v_1 &= \alpha_1 \cdot v_1 - v_{1set} \\ \Delta T &= T_1 - T_{set} \quad (29)\end{aligned}$$

where  $\alpha_1$  is a static error coefficient to reduce the static error between the measured value and the true value of  $v_1$ . Because the evaluation criterion of the application result of this project is the value of  $\Delta T$ , it is assumed that the measurement of  $T_1$  has no static error, and the dynamic error is extremely small, so that only static error adjustment is performed on  $v_1$ .

By adjusting the equation (29), the calculate  $s$  can more accurately reflect the system state.

2) The  $x_3$  in the control law (28) can be written as follows

$$\begin{aligned}x_3 &= \frac{k \cdot v_3 \cdot j_1 \cdot J_1}{L \cdot R_1(t)} \cdot \Delta T + \frac{k \cdot (E \cdot A - T_0) \cdot j_1 \cdot J}{L \cdot R_1(t)} \cdot \Delta v_1 \\ &= c_1 \cdot \Delta T + c_2 \cdot \Delta v_1\end{aligned}$$

In order to make  $\Delta T$  and  $\Delta v_1$  have a considerable adjustment effect on the system to reduce the influence of the error on the system, the value of  $k$  cannot be too small. In this experiment we have  $k = -0.1$ , and when the large-diameter diaphragm roll is unwinding,  $c_2 < -3 \times 10^4$ , the excessive coefficient  $c_2$  before  $\Delta v_1$  will cause the measurement error to be amplified. If the error amplified by  $c_2$  directly acts on the motor torque control, which will cause excessive system damage.

To solve these problems, a fault-tolerant sliding mode controller (FSMC) is proposed, which improves the fault tolerance of  $x_3$  in the (28), as follow

$$x_3 = k \cdot \left( \frac{\Delta T}{L} \cdot v_3 + \frac{E \cdot A \cdot \Delta v_1}{\alpha_2 \cdot L} - \frac{\Delta v_1}{L} \cdot T_0 \right) \cdot \frac{j_1 \cdot J_1}{R_1(t)} \quad (30)$$

where  $\alpha_2 > 1$  is the fault tolerance coefficient, which is used to reduce the adverse effect of measurement error on control.

## IV. DESIGN OF DIFFERENTIAL TRACKING DISTURBANCE OBSERVER

Delay in hardware and discontinuous switching of the controller will cause chattering of the control. To reduce chattering, one method is to use a continuous saturation function or sigmoid function to approximate the discontinuous symbol function in the controller [26], [27], but this method will produce large steady-state errors due to the boundary layer around the sliding surface [21]. Another method is to reduce the switching gain, that is reduce the  $\varepsilon$  in the trending law (20). However, there are mismatched interferences in many practical systems [28]. In general, when the external disturbance is large, in order to enhance the actual robustness of the system, it is necessary to increase the switching gain  $\varepsilon$  in (20), but this will result in a larger control chattering. Therefore, in order to improve the robustness of the system while reducing the chattering of the control, the disturbance observer is used to estimate the disturbance in the system based on the control of the diaphragm tension by the sliding mode controller, and then compensated in the control signal.

The disturbance observer is an inner-loop controller, which can compensate the uncertainty and external disturbance of the system and make the inner-loop behavior conform to the established nominal model, that is, the outer-loop controller deals with nominal stability and nominal performance, and the inner loop DOB improves robustness against uncertainty and disturbances [29].

The general disturbance observer based on nominal model(DOB) is shown in the red box, as follow

In the picture,  $P(s)$  is the model of the system.  $P_n^{-1}(s)$  is the inverse model of the nominal model,  $Q(s)$  is low-pass filter,

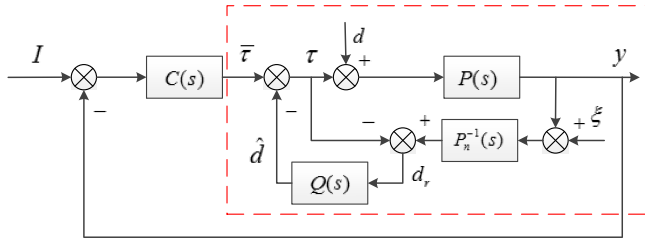


**FIGURE 4.** Disturbance observer based on nominal model.

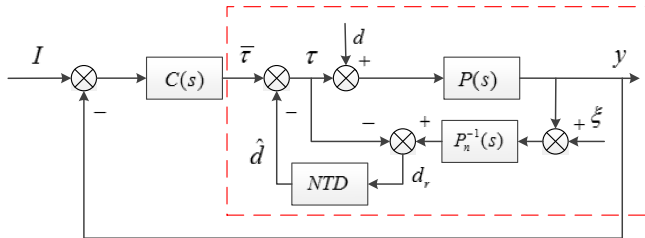


**FIGURE 5.** Differential tracking disturbance observer based on differential tracker.

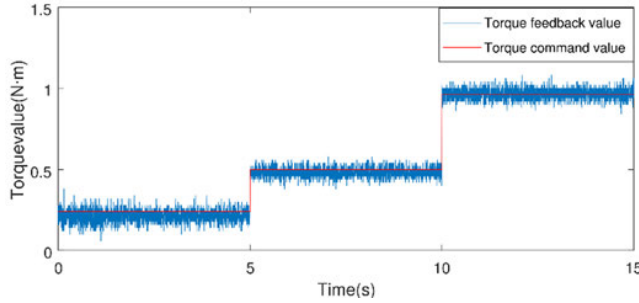


**FIGURE 6.** Torque control and feedback.

$\xi$  is measuring noise,  $C(s)$  is outer-loop controller,  $I$  is input signal of outer-loop controller,  $d$  is actual disturbance to the system,  $d_r$  is unfiltered disturbance estimate. The estimated disturbance is as follow

$$\hat{d} \approx Q(s)\{[(\tau + d)P(s)]P_n^{-1}(s) - \tau\}$$

Although the low-pass filter can reduce the influence of the measurement noise on the disturbance estimation, it will cause the phase lag of the disturbance estimation, and the excessive lag will increase the control chattering in engineering applications.

For the problem of lag, this paper proposes a differential tracking disturbance observer (DTDO) based on nonlinear differential tracker (NTD), its control block diagram is shown in the figure below.

The basic form of the differential tracker is as follows

$$\begin{cases} \dot{z}_1(t) = z_2(t), & z_1(0) = z_{10} \\ \dot{z}_2(t) = \Re^2 f \left[ z_1(t) - d_r(t), \frac{z_2(t)}{\Re} \right], & z_2(0) = z_{20} \end{cases}$$

Its convergence is proved in [30]. Where parameter  $\Re > 0$ ,  $f : \mathbb{R}^2 \rightarrow \mathbb{R}$  is a local Lipschitz continuous function,  $(z_{10}, z_{20})$  is any initial value. By constructing  $f$ , the state variable  $z_1$  can track the input signal  $d_r$ , and the state variable  $z_2$  is the approximate differential of the input signal.

To reduce the hysteresis of the differential tracker, this paper uses the improved scheme of the above differential tracker in [31], as follow.

$$\begin{cases} \dot{z}_1(t) = z_2(t), & z_1(0) = z_{10}, z_2(0) = z_{20} \\ \dot{z}_2(t) = \Re^2 f \left[ z_1(t) - d_r(t), \frac{z_2(t)}{\Re} \right] + \alpha_3 \dot{d}_r(t) \end{cases} \quad (31)$$

where the feedforward gain  $\alpha_3 > 0$ , the feedforward  $\alpha_3 \dot{d}_r(t)$  can speed up the tracking of the input signal  $d_r$  by the state variable  $z_1$ .

The  $f$  function uses a combination of power functions [31], as follow

$$f(Z_1, Z_2) = -\alpha_4 \left[ (\alpha_5 Z_1)^{\frac{p}{q}} + Z_1 \right] - \alpha_6 \left[ (\alpha_5 Z_2)^{\frac{p}{q}} + Z_2 \right] \quad (32)$$

where  $\alpha_4 > 0$ ,  $\alpha_5 \geq 1$ ,  $\alpha_6 > 0$ ,  $p > q > 0$ ,  $p$  and  $q$  are both odd numbers which decide the shape of  $f$ .

Although the derivative  $\dot{d}_r(t)$  of the input signal appears in equation (32), it is not required in the calculation of  $z_2$ .

$$\begin{aligned} z_2 &= \Re^2 \int_0^t \left[ \bar{z}_1(\iota) - d_r(\iota), \frac{\bar{z}_2(\iota)}{\Re} \right] d\iota + \alpha_3 [d_r(t) - d_r(0)] + z_{20} \\ z_1 &= \int_0^t \bar{z}_2(\iota) d\iota + z_{10} \end{aligned}$$

where  $\bar{z}_1$  and  $\bar{z}_2$  is the old value of  $z_1$  and  $z_2$ .

The integral calculation from  $d_r$  to  $z_2$  can effectively filter the noise, and the  $z_1$  calculated by  $z_2$  can not only effectively filter the noise in  $d_r$ , but also reduce the hysteresis between  $z_1$  and  $d_r$ , so that the tracking of  $z_1$  to  $d_r$  is more real-time and accurate, thereby improving the robustness and disturbance tracking performance of the disturbance observer.

In this paper, the unfiltered disturbance  $d_r$  calculated based on the nominal model is used as the input signal of DTDO, and the state variable  $z_1$  of the tracking input in DTDO is taken as the output of DTDO, that is, the final compensation for output of FSMC.

## V. EXPERIMENT

There are two extreme operating conditions in the operation of the LBDMS, namely low speed transmission and high speed transmission of the diaphragm. The experiments in this paper are mainly for the former. In order to verify the actual control performance of the designed FSMCDTDOC on the diaphragm tension of the unwinding system, a comparison experiment between FSMCDTDOC and FSMC, PID controller (PIDC), and fault-tolerant sliding mode controller with compensation of general disturbance observer (FSMCDOB) was carried out. In the experiment, the PLC operating cycle is 1ms, and the parameters used in the experiment are:

$$\begin{aligned} r_1 &= 0.0465m; \quad E = 1.2929 \times 10^9 N/m^2; \quad H = 0.109m; \\ a_3 &= 1.885 m/s^2; \quad h = 0.00002m; \quad J_c = 0.0102 kg \cdot m^2; \end{aligned}$$

**TABLE 1.** Torque control performance.

Expectation(N·m)	0.24	0.5	0.96
Maximum	0.38	0.58	1.08
Minimum	0.06	0.38	0.84
Mean	0.2132	0.4818	0.9653
Mode	0.22	0.48	0.96
Standard deviation	0.03768	0.02969	0.03358
Range	0.32	0.2	0.24
Maximum relative error	-0.18	-0.12	$\pm 0.12$
Maximum absolute error	-75%	-24%	$\pm 12.5\%$

**TABLE 2.** PID control effect of  $v_3$ .

Expectation(m/s)	0.1	0.2	0.3
Maximum	0.106	0.2087	0.3081
Minimum	0.09289	0.1937	0.2918
Mean	0.09999	0.2	0.3
Mode	0.09771	0.1976	0.2982
Standard deviation	0.002256	0.001828	0.001886
Range	0.01315	0.01504	0.01628
Maximum relative error	-0.00711	+0.0087	-0.0082
Maximum absolute error	-7.11%	-4.35%	+2.733%

$$J_m = 0.000198 \text{ kg} \cdot \text{m}^2; \quad \rho = 541.45487 \text{ kg/m}^3;$$

$$j_1 = 1; \quad L = 0.57 \text{ m}; \quad b_1 = 0.056; \quad k = -0.1, \quad \varepsilon = 0.01,$$

$$\beta = 1; \quad \alpha_1 = 0.96; \quad \alpha_2 = 0.14; \quad \alpha_3 = 12; \quad \alpha_4 = 1;$$

$$\alpha_5 = 2; \quad \alpha_6 = 2; \quad p = 33; \quad q = 31; \quad \Re = 3.5.$$

The proportional gain  $K_p = 45$ , integration time constant  $K_i = 0.4$ , and differential time constant  $K_d = 0.05$  in PIDC;  $\varepsilon = 0.08$  in FSMC and FSMCDOB; The friction torque  $Md_1$  is initially determined as:

$$Md_1 = -7.747 \times 10^{-5} \omega_1^2 + 0.012\omega_1 + 0.12$$

The experiment is based on the torque control of the servo. The torque control performance of the servo used as follow.

The PID control effect of  $v_3(\text{m/s})$  during the experiment is shown in the following table.

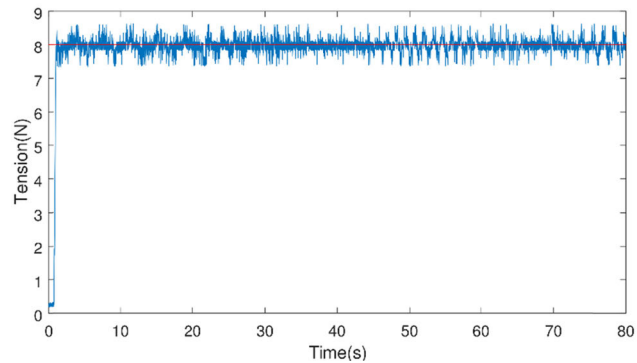
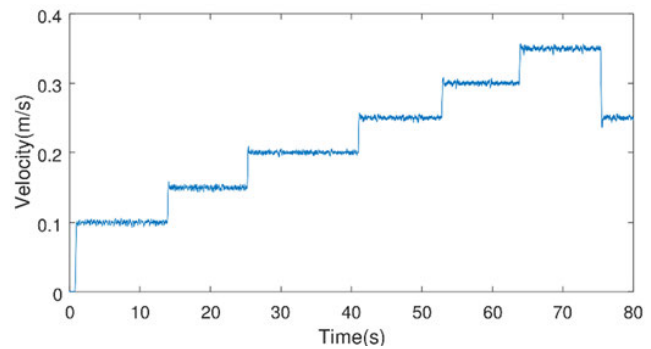
#### A. SPEED RESPONSE EXPERIMENT

In this experiment, the control effects of different controllers on the diaphragm tension in the unwinding system under the same expected tension  $T_{set} = 8N$  and different transmission speeds ( $v_3 = 0.1 \text{ m/s}$  to  $0.35 \text{ m/s}$ , interval  $0.05 \text{ m/s}$ ) are tested. And repeated experiment under  $v_3 = 0.25 \text{ m/s}$ , as follow.

From the comparison of Fig.7, Fig.9, Fig.11, and Fig.12 and the data in Table 3, the FSMDTDOC exhibits the best control performance of the diaphragm tension in all indexes after the system is started. The tracking error is small, the control performance of the acceleration process is good, and the rise time is  $0.494\text{s}$ , which is less than the rise time  $1.713\text{s}$  of the PIDC. It can be seen from Fig. 15 that the designed DTDO can not only filter the disturbance (the blue line in the figure) directly calculated by the nominal model, but also the observed disturbance phase lag is small, the

**TABLE 3.** Tension control of different controllers at different speeds.

Controller	FSMCDT DOC	PIDC	FSMC	FSMCDOB
Expectation (N)	8	8	8	8
Minimum	7.331	4.372	5.5	2.162
Maximum	8.636	13.04	10.3	12.88
Mean	7.981	7.913	7.799	7.881
Standard deviation	0.208	0.5889	0.646	2.062
Range	1.305	8.672	4.799	10.71
Maximum relative error	-0.663	+5.04	-2.5	-5.838
Maximum absolute error	+8.2875%	+63%	31.25%	72.975%

**FIGURE 7.** Tension control effect of FSMDTDOC at different speeds.**FIGURE 8.**  $v_3$  in the FSMDTDOC experiment.

tracking effect is good, and the overall control performance of the FSMDTDOC is improved. PIDC performs poorly during acceleration and deceleration. The maximum tension error occurs in the acceleration process, and there is a large steady-state error in the repeated experiment of transmission speed  $v_3 = 0.25 \text{ m/s}$ . The difference between the average values of the tension before and after is  $0.324 \text{ N}$ , which is greater than  $0.0936 \text{ N}$  of FSMDTDOC. The average tension under FSMC control is  $7.799$ , which is not much different from the expected tension, and the control performance during acceleration is better than PIDC. However, due to the lack of disturbance compensation, the chatter of tension in the control process is large. Due to the hysteresis of disturbance

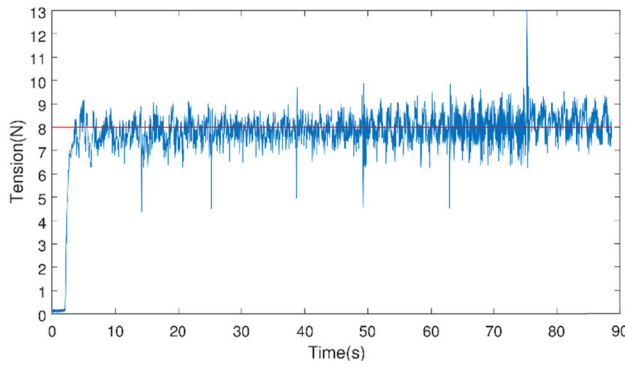


FIGURE 9. Tension control effect of PIDC at different speeds.

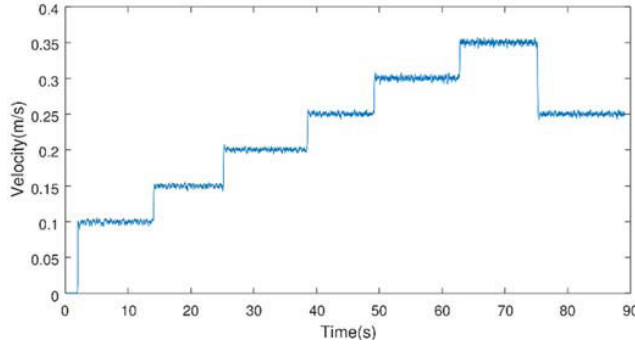
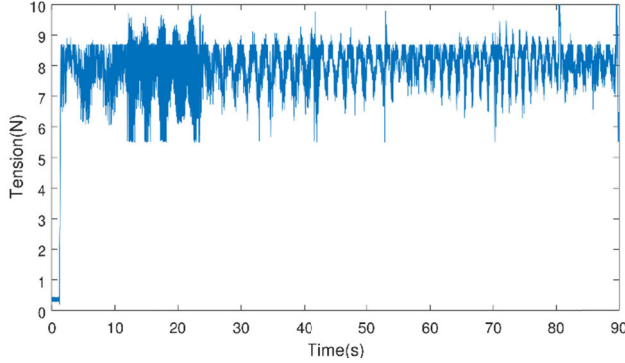
FIGURE 10.  $v_3$  in the PIDC experiment.

FIGURE 11. Tension control effect of FSMC at different speeds.

compensation, FSMCDOB intensifies the disturbance of the system and causes large diaphragm tension control error.

#### B. EXPECTED TENSION RESPONSE EXPERIMENT

In this experiment, the control effect of FSMCDTDOC and PIDC on diaphragm tension in unwinding system under the same transmission speed ( $v_3 = 0.25\text{m/s}$ ) and different expected tension ( $T_{set} = 2\text{N}, 4\text{N}, 6\text{N}, 8\text{N}$ ) are tested.

From the comparison of Fig. 16 and Fig. 17, and the data in Table 4, FSMCDTDOC is still better than PIDC for different desired tension control. But the maximum absolute error of both is very large, which is related to the servo torque control performance. The maximum absolute error of FSMDTDOC and PIDC in Table 4 appears in the control of  $T_{set} = 2\text{N}$ . It can be seen from Figures 18 and 19 that the required unwinding motor torque is small, and the servo used in this

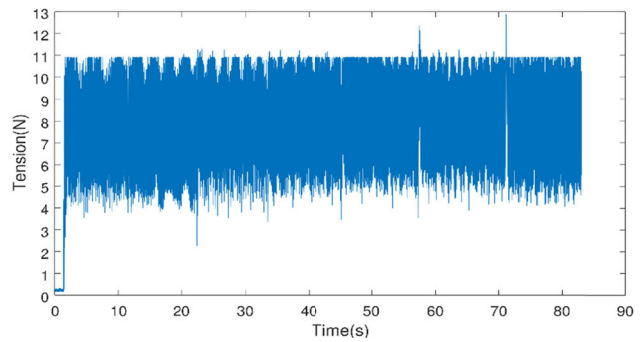


FIGURE 12. Tension control effect of FSMCDOB at different speeds.

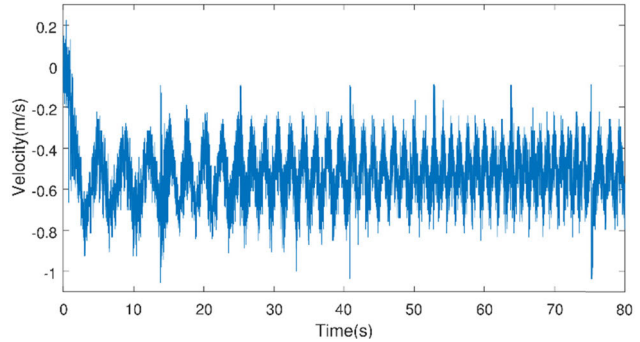


FIGURE 13. Motor output torque of FSMCDTDOC at different speeds.

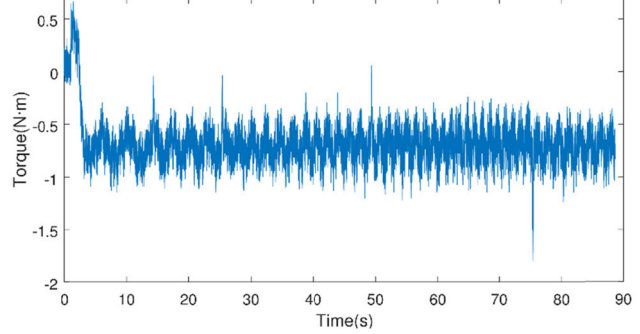


FIGURE 14. Motor output torque of PIDC at different speeds.

TABLE 4. Control effects of different controllers on different expected tensions.

Controller	FSMCDTDOC	PIDC
Maximum relative error	+0.764	+1.567
Maximum absolute error	+38.2%	+62.5%

paper has a poor control effect on small torque values (see Table 1), which directly leads to poor tension control. It can be seen from Fig. 20 that the DTDO designed in this paper still shows good filtering and tracking effect on the disturbance.

#### C. GENERALIZATION EXPERIMENT

In order to verify the generalization ability of the same control parameters of the controller, this experiment carried out the diaphragm tension control experiment of medium

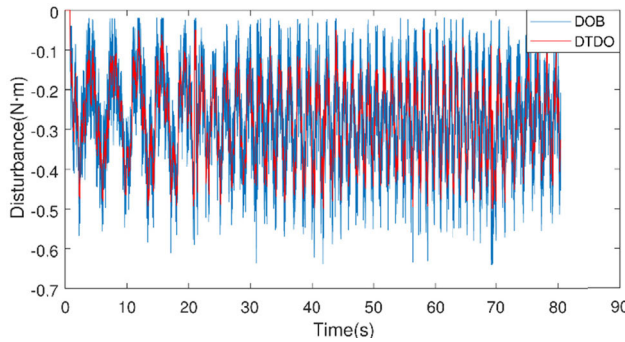


FIGURE 15. Observed disturbance of FSMCDTDOC at different speeds.

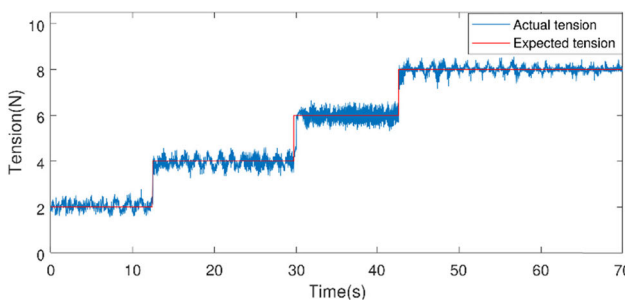


FIGURE 16. Control effects of different tensions of FSMCDTDOC.

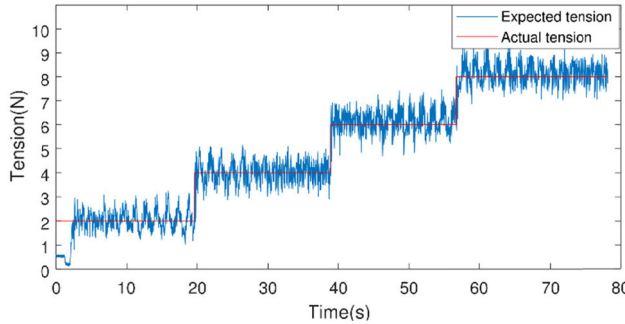


FIGURE 17. Control effects of different tensions of PID.

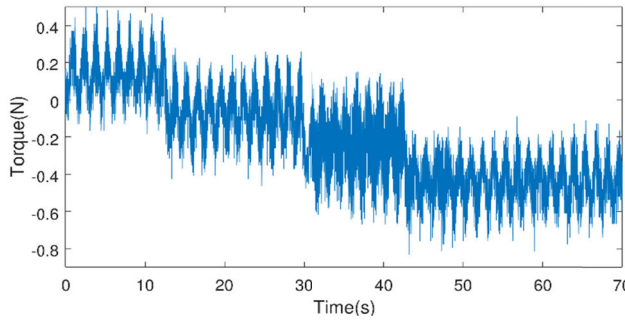


FIGURE 18. Motor output torque of FSMCDTDOC for different tension control.

transmission speed ( $v_3 = 0.6m/s$  to  $1m/s$ , interval  $0.1m/s$ ) of  $T_{set} = 8N$  based on the controller control parameters in the above experiment. The experimental results are as follows.

Comparing Fig. 21 with Fig. 22, it can be seen that the generalization ability and stability of FSMDTDOC are

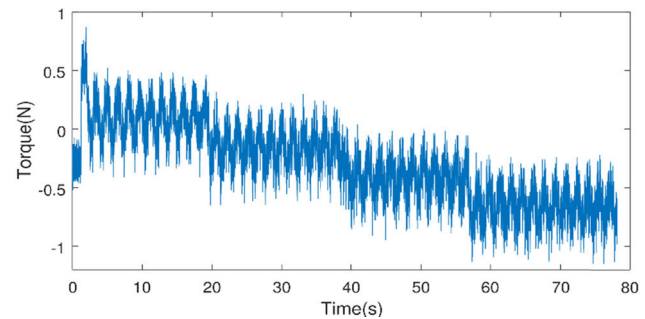


FIGURE 19. Motor output torque of PID for different tension control.

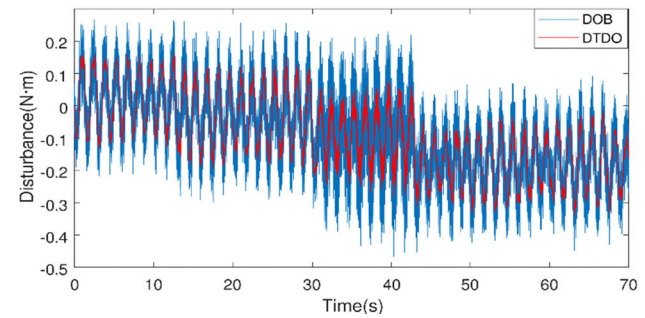


FIGURE 20. Observed disturbance of different tension controls of FSMCDTDOC.

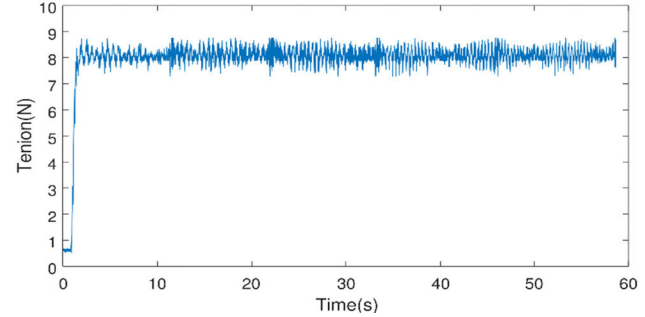


FIGURE 21. The tension control effects of different medium speed of FSMCDTDOC.

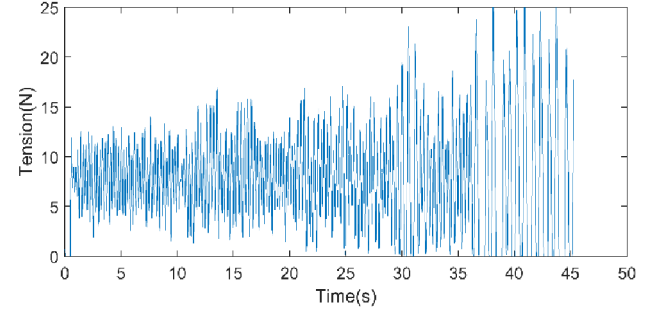


FIGURE 22. The tension control effects of different medium speed of PIDC.

much stronger than PIDC when the control parameters are unchanged.

Based on the above comparative experiments, the FSMDTDOC designed in this paper has a faster rising speed, less tracking error, stable acceleration and deceleration, and better

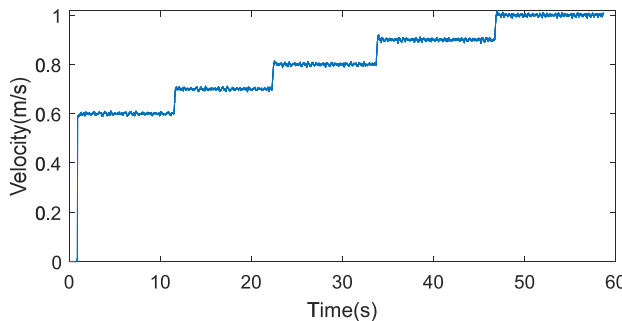


FIGURE 23.  $v_3$  in medium speed experiment of FSMDTDOC.

overall control performance, which can be better applied to practical engineering applications.

## VI. CONCLUSION

A FSMDTDOC is proposed in this paper for the unwinding system of LBDSM in practical applications. The final comparison experiment confirms the good control performance of the proposed FSMDTDOC in practical engineering applications - fast rising speed, small tracking error, strong generalization ability, good acceleration and deceleration performance and stability.

## REFERENCES

- [1] V. Gassmann, D. Knittel, P. R. Pagilla, and M.-A. Bueno, “H $\infty$  unwinding Web tension control of a strip processing plant using a pendulum dancer,” in *Proc. IEEE Amer. Control Conf.*, Jun. 2009, pp. 901–906.
- [2] P. R. Pagilla, N. B. Siraskar, and R. V. Dwivedula, “Decentralized control of Web processing lines,” *IEEE Trans. Control Syst. Technol.*, vol. 15, no. 1, pp. 106–117, Jan. 2007.
- [3] F. Sell-Le Blanc, J. Hofmann, R. Simmler, and J. Fleischer, “Coil winding process modelling with deformation based wire tension analysis,” *CIRP Ann.*, vol. 65, no. 1, pp. 65–68, 2016.
- [4] M. Baumgart and L. Pao, “Time-optimal control of Web-winding systems with air entrainment,” *IEEE/ASME Trans. Mechatronics*, vol. 10, no. 3, pp. 257–262, Jun. 2005.
- [5] L. P. Perera, “The role of active dancers in tension control of Webs,” M.S. thesis, Web Handling Res. Center, Oklahoma State Univ., Stillwater, OK, USA, 2001, pp. 227–242.
- [6] P. Pagilla, S. Garimella, L. Dreinhoefer, and E. King, “Dynamics and control of accumulators in continuous strip processing lines,” *IEEE Trans. Ind. Appl.*, vol. 37, no. 3, pp. 934–940, May/Jun. 2001.
- [7] P. R. Pagilla, R. V. Dwivedula, Y. Zhu, and L. P. Perera, “Periodic tension disturbance attenuation in Web process lines using active dancers,” *J. Dyn. Syst., Meas., Control*, vol. 125, no. 3, pp. 361–371, Sep. 2003.
- [8] R. V. Dwivedula, Y. Zhu, and P. R. Pagilla, “Characteristics of active and passive dancers: A comparative study,” *Control Eng. Pract.*, vol. 14, no. 4, Apr. 2006, Art. no. 409423.
- [9] T. Sakamoto and T. Kobayashi, “Decomposition and decentralized controller design of Web transfer system,” *IFAC Proc. Volumes*, vol. 37, no. 11, pp. 135–140, Jul. 2004.
- [10] D. Knittel, E. Laroche, D. Gigan, and H. Koc, “Tension control for winding systems with two-degrees-of-freedom H $\infty$  controllers,” *IEEE Trans. Ind. Appl.*, vol. 39, no. 1, pp. 113–120, Jan. 2003.
- [11] H. Koc, D. Knittel, M. De Mathelin, and G. Abba, “Modeling and robust control of winding systems for elastic Webs,” *IEEE Trans. Control Syst. Technol.*, vol. 10, no. 2, pp. 197–208, Mar. 2002.
- [12] J. Li, X. Mei, T. Tao, and S. Liu, “Design tension controller of unwinding system based on BP neural network,” *Adv. Sci. Lett.*, vol. 4, no. 6, pp. 2222–2226, 2011.
- [13] K. Choi, M. Zubair, and G. Ponniah, “Web tension control of multi-span roll-to-roll system by articial neural networks for printed electronics,” *Proc. Inst. Mech. Eng., C, J. Mech. Eng. Sci.*, vol. 227, no. 10, pp. 2361–2376, 2013.
- [14] A. Benlatreche, D. Knittel, and E. Ostertag, “Robust decentralised control strategies for large-scale Web handling systems,” *Control Eng. Pract.*, vol. 16, no. 6, pp. 736–750, 2008.
- [15] W. Zhou and Z. Gao, “An active disturbance rejection approach to tension and velocity regulations in Web processing lines,” in *Proc. IEEE 22nd Int. Symp. Intell. Control*, Oct. 2007, pp. 842–848.
- [16] K. Chin Lin, “Observer-based tension feedback control with friction and inertia compensation,” *IEEE Trans. Control Syst. Technol.*, vol. 11, no. 1, pp. 109–118, Jan. 2003.
- [17] K. C. Lin, M. C. Tsai, and K. Y. Chen, “Web tension control of a start-up process using observer techniques with friction and inertia compensation,” in *Proc. 27th Annu. Conf. IEEE Ind. Electron. Soc.*, Nov. 2001, pp. 529–534.
- [18] S. Garimella and K. Srinivasan, “Application of iterative learning control to coil-to-coil control in rolling,” *IEEE Trans. Control Syst. Technol.*, vol. 6, no. 2, pp. 281–293, Mar. 1998.
- [19] J.-S. Lu, M.-Y. Cheng, K.-H. Su, and M.-C. Tsai, “Wire tension control of an automatic motor winding machine—An iterative learning sliding mode control approach,” *Robot. Comput.-Integr. Manuf.*, vol. 50, pp. 50–62, Apr. 2018.
- [20] S. Y. Shao, M. Chen, and Q. X. Wu, “Stabilization control of continuous-time fractional positive systems based on disturbance observer,” *IEEE Access*, vol. 4, pp. 3054–3064, 2016.
- [21] S.-L. Shi, J.-X. Li, and Y.-M. Fang, “Extended-state-observer-based chattering free sliding mode control for nonlinear systems with mismatched disturbance,” *IEEE Access*, vol. 6, pp. 22952–22957, 2018.
- [22] P. Yang, X. Ma, J. Wang, G. Zhang, Y. Zhang, and L. Chen, “Disturbance observer-based terminal sliding mode control of a 5-DOF upper-limb exoskeleton robot,” *IEEE Access*, vol. 7, pp. 62833–62839, 2019.
- [23] H. Q. Tian, “Sliding mode control theory and application,” *Wuhan Press*, vol. 1995, pp. 1–5.
- [24] H. K. Khalil, “Nonlinear design tool,” in *Nonlinear Systems*. Beijing, China: Publishing House of Electronics Industry, 2017, pp. 330–430.
- [25] J.-K. Liu and F.-C. Sun, “Research and development on theory and algorithms of sliding mode control,” *Control Theory Appl.*, vol. 24, no. 3, pp. 407–418, Jun. 2007.
- [26] M. Benosman and K.-Y. Lum, “Passive actuators’ fault-tolerant control for affine nonlinear systems,” *IEEE Trans. Control Syst. Technol.*, vol. 18, no. 1, pp. 152–163, Jan. 2010.
- [27] L. Yang and J. Yang, “Nonsingular fast terminal sliding-mode control for nonlinear dynamical systems,” *Int. J. Robust Nonlinear Control*, vol. 21, no. 16, pp. 1865–1879, Nov. 2011.
- [28] C.-C. Hua and X.-P. Guan, “Smooth dynamic output feedback control for multiple time-delay systems with nonlinear uncertainties,” *Automatica*, vol. 68, pp. 1–8, Jun. 2016.
- [29] H. Shim, G. Park, Y. Joo, J. Back, and N. H. Jo, “Yet another tutorial of disturbance observer: Robust stabilization and recovery of nominal performance,” *Control Theory Technol.*, vol. 14, no. 3, pp. 237–249, Aug. 2016.
- [30] B.-Z. Guo and Z.-L. Zhao, “On convergence of tracking differentiator,” *Int. J. Control.*, vol. 84, no. 4, pp. 693–701, Apr. 2011.
- [31] D. Tian, H. Shen, and M. Dai, “Improving the rapidity of nonlinear tracking differentiator via feedforward,” *IEEE Trans. Ind. Electron.*, vol. 61, no. 7, pp. 3736–3743, Jul. 2014.



**CHENG JIANG** received the B.E. degree in mechatronic engineering from Hunan Agricultural University, in 2017. He is currently pursuing the M.E. degree in mechanical engineering with Central South University. His research interests include mechatronics control and robot control.



**HENG-SHENG WANG** received the Ph.D. degree in mechanical and (electrical) engineering from Central South University, in 2006. He joined Central South University, in 2000, where he has been teaching control theory and (measurement) technology in the field of mechanical engineering. His research interests include dynamics and control of mechanical systems, industrial manipulators, mobile robotics, and applications of artificial intelligence.



**LIANG-LIANG JIANG** received the B.E. degree in mechanical engineering from Central South University, in 2018, where he is currently pursuing the M.E. degree in mechanical engineering. His research interests include mechatronics control and robot control.

• • •



**LI-WEI HOU** received the M.E. degree in mechanical engineering from Tianjin University, in 2017. He is currently pursuing the Ph.D. degree in mechanical engineering with Central South University. His research interests include robot force control and learning based on manipulation.